Long-Term Course and Mutational Spectrum of *spatacsin*-Linked Spastic Paraplegia

Ute Hehr, MD,[1] Peter Bauer, MD,[2] Beate Winner, MD,[3] Rebecca Schule, MD,[4] Akguen Olmez, MD,[5] Wolfgang Koehler, MD,[6] Goekhan Uyanik, MD,[3] Anna Engel, MSc,[2] Daniela Lenz, MSc,[2] Andrea Seibel, MSc,[4] Andreas Hehr, PhD,[1] Sonja Ploetz, MSc,[3] Josep Gamez, MD,[7] Arndt Rolfs, MD,[8] Joachim Weis, MD,[9] Thomas M. Ringer, MD,[10] Michael Bonin, PhD,[2] Gerhard Schuierer, MD,[11] Joerg Marienhagen, MD,[12] Ulrich Bogdahn, MD,[3] Bernhard H. F. Weber, PhD,[1] Haluk Topaloglu, MD,[5] Ludger Schols, MD,[4] Olaf Riess, MD,[2] and Juergen Winkler, MD[3]

Objective: Hereditary spastic paraplegias (HSPs) comprise a heterogeneous group of neurodegenerative disorders resulting in progressive spasticity of the lower limbs. One form of autosomal recessive hereditary spastic paraplegia (ARHSP) with thin corpus callosum (TCC) was linked to chromosomal region 15q13-21 (SPG11) and associated with mutations in the *spatacsin* gene. We assessed the long-term course and the mutational spectrum of *spatacsin*-associated ARHSP with TCC.

Methods: Neurological examination, cerebral magnetic resonance imaging (MRI), ^{18}fluorodeoxyglucose positron emission tomography (PET), nerve biopsy, linkage and mutation analysis are presented.

Results: Spastic paraplegia in patients with *spatacsin* mutations (n = 20) developed during the second decade of life. The Spastic Paraplegia Rating Scale (SPRS) showed severely compromised walking between the second and third decades of life (mean SPRS score, >30). Impaired cognitive function was associated with severe atrophy of the frontoparietal cortex, TCC, and bilateral periventricular white matter lesions. Progressive cortical and thalamic hypometabolism in the ^{18}fluorodeoxyglucose PET was observed. Sural nerve biopsy showed a loss of unmyelinated nerve fibers and accumulation of intraaxonal pleomorphic membranous material. Mutational analysis of *spatacsin* demonstrated six novel and one previously reported frameshift mutation and two novel nonsense mutations. Furthermore, we report the first two splice mutations to be associated with SPG11.

Interpretation: We demonstrate that not only frameshift and nonsense mutations but also splice mutations result in SPG11. Mutations are distributed throughout the *spatacsin* gene and emerge as major cause for ARHSP with TCC associated with severe motor and cognitive impairment. The clinical phenotype and the ultrastructural analysis suggest a disturbed axonal transport of long projecting neurons.

Ann Neurol 2007;62:656–665

Hereditary spastic paraplegia (HSP) genetically comprises one of the most heterogeneous groups of monogenetic neurodegenerative disorders. The mode of inheritance is autosomal dominant, autosomal recessive, or X-linked. To date, 36 distinct HSP loci designated SPG (spastic paraplegia) have been assigned with 15 disease-associated genes identified so far.[1] The diversity of HSP loci indicates a complex genetic control for the function of motor neurons and their axonal projections. The HSP genes encode proteins with diverse cellular functions associated with mitochondria (eg, SPG7, SPG13), axonal transport (eg, SPG3A, SPG4, SPG10), myelinization (eg, SPG2), or development of the corticospinal tract (CST; eg, SPG1).[1,2] An axonal dying back of long-projecting motor neurons is one potential mechanism underlying the CST degenera-

From the [1]Department of Human Genetics, University of Regensburg, Regensburg; [2]Department of Medical Genetics, University of Tuebingen, Tuebingen; [3]Department of Neurology, University of Regensburg, Regensburg; [4]Research Division for Clinical Neurogenetics, Centre of Neurology and Hertie-Institute for Clinical Brain Research, University of Tuebingen, Tuebingen, Germany; [5]Department of Pediatric Neurology, Hacettepe University, Ankara, Turkey; [6]Department of Neurology, Fachkrankenhaus Hubertusburg, Wermsdorf, Germany; [7]Department of Neurology, Hospital General Vall d'Hebron, Barcelona, Spain; [8]Department of Neurology, University of Rostock, Rostock; [9]Institute of Neuropathology, Rheinisch-Westfälische Technische Hochschule of Aachen, Aachen; [10]Department of Neurology, University of Jena, Jena; [11]Institute of Neuroradiology, Bezirksklinikum Regensburg; and [12]Department of Nuclear Medicine, University of Regensburg, Regensburg, Germany.

Received Jul 20, 2007, and in revised form Oct 9. Accepted for publication Oct 26, 2007.

U.H., P.B., B.W., and R.S. contributed equally to this work.

Published online Dec 7, 2007, in Wiley InterScience (www.interscience.wiley.com). DOI: 10.1002/ana.21310

Address correspondence to Dr Winkler, Department of Neurology, University of Regensburg, Universitaetsstrasse 84, D-93053 Regensburg, Germany. E-mail: juergen.winkler@klinik.uni-regensburg.de

tion. Neuropathological analysis of the spinal cord, rarely performed in HSP, showed axonal degeneration most marked in the distal terminals of CST and *fasciculus gracilis* projections.[3]

Recently, progress has been made to establish a rating scale for HSP (Spastic Paraplegia Rating Scale [SPRS]) as an important clinical tool to assess severity and natural course of HSP.[4] Clinically, pure and complicated forms of HSP are distinguished.[5] Pure forms present with clinical features of pyramidal motor neuron dysfunction such as spastic weakness of the lower limbs and are often accompanied by urinary urgency and subtle dorsal column impairment.[1] However, clinical and neuroimaging parameters currently fail to distinguish between the different genetic forms of pure HSP. In contrast, complicated forms are characterized by additional nonpyramidal signs and symptoms, and are associated with additional structural abnormalities of the central nervous system (CNS) such as thin corpus callosum (TCC), white matter (WM) lesions, and cortical and/or cerebellar atrophy. In addition, neurological symptoms such as neuropathy, amyotrophy, ataxia, extrapyramidal motor signs, epilepsy, or cognitive deficits are observed. Furthermore, other organs may also be affected (eg, cataracts, skeletal abnormalities).[1]

A clinically distinct form of autosomal recessive hereditary spastic paraplegia (ARHSP) with TCC has been linked to the long arm of chromosome 15 at 15q13-15 and designated SPG11.[6–8] SPG11 is characterized by progressive spasticity of the lower limbs, TCC, cognitive impairment, and severe neuropathy.[9,10] We have recently linked four large consanguineous Turkish families to this region.[11] Based on the presence of two recombination events, we refined the SPG11 critical region to a 2.93 cM interval with a maximum LOD score of 11.84.[11] Within this candidate interval, *KIAA1840* was recently identified as the *spatacsin* gene associated with SPG11 and appears to be the most frequent cause for ARHSP with TCC.[12]

By sequencing the entire coding region of the *spatacsin* gene, we identified 1 previously reported and 10 novel *spatacsin* mutations in 3 consanguineous pedigrees from Turkey, 1 from Saudi Arabia, and 1 from Germany, linked to SPG11, and in 4 sporadic patients from Germany and Spain. Our data demonstrate that frameshift and nonsense mutations, as well as splice mutations, result in the SPG11 phenotype. Furthermore, we assess the phenotype and natural long-term course of these *spatacsin*-associated HSP patients.

Patients and Methods

Minimal inclusion criteria for this patient cohort were: (1) family history compatible with an autosomal recessive inheritance, (2) progressive spasticity of the lower limbs, (3) TCC, and (4) cognitive impairment in at least one index patient of each family. Detailed neurological examination of 18 patients from 9 families with suspected SPG11 was performed applying the SPRS. This scale measures disease severity consisting of a 13-item scale to rate functional impairment.[4] Some of these patients were continuously treated for up to 10 years. Diagnostic workup included comprehensive laboratory analysis (cerebrospinal fluid for the presence of oligoclonal bands, blood testing for electrolytes, hormones, very long chain fatty acids, fats, vitamins, and infectious diseases) and screening tests for mitochondrial dysfunction (lactate and pyruvate before and after glucose loading[13]), and tandem mass spectra analysis of acylcarnitine (C16:0+C18:1/C2 ratio[14]). Neuroradiological evaluation included long-term follow-up of cerebral and spinal magnetic resonance imaging (MRI) in three patients. A single-voxel ^{1}H-proton magnetic resonance spectroscopy (TE/TR 272/2,000 milliseconds from frontal and parietooccipital brain regions, centrum semiovale, and internal capsule) was performed in one patient. Long-term follow-up ^{18}fluorodeoxyglucose positron emission tomography (FDG-PET) images were obtained for three patients. Histological and ultrastructural evaluation was performed for one sural nerve biopsy.

Peripheral blood samples for the genetic analysis were obtained and clinical data included after informed consent of the patients or parents, respectively, according to bioethical laws for research on human subjects. DNA was extracted from whole EDTA blood using standard protocols. The coding exons and the intron exon boundaries of 30 genes (*CHST14, DLL4, GANC, GCHFR, GCP4, CTDSPL2, IT-*

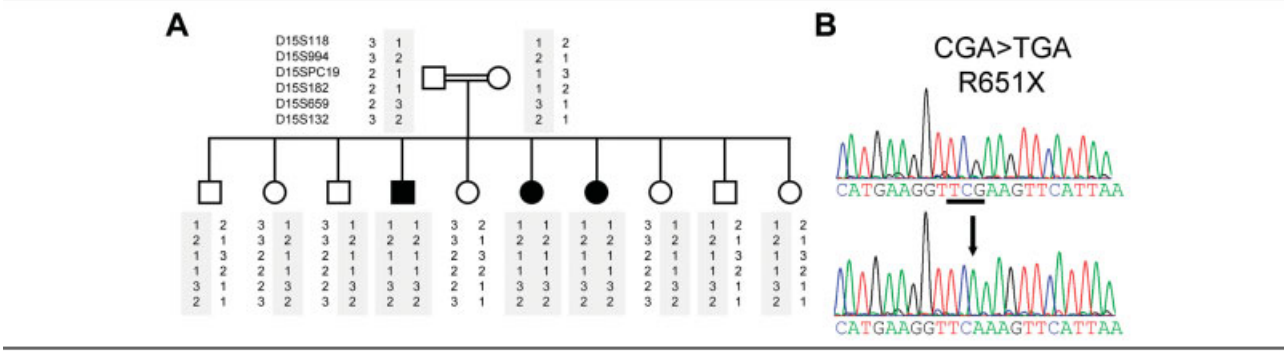

Fig 1. (A) Linkage of the consanguineous Saudi-Arabian family (F5) to SPG11 and (B) reverse sequence of exon 10 of index proband P5_3 with homozygous base substitution CGA>TGA, resulting in the nonsense mutation R651X.

Table 1. **Summary of Spatacsin Mutations**

Location	Family[a] ID[Origin]	Zygosity	Mutation acc. to NM_025137 (cDNA)	Amino Acid Substitution	Reference
Exon 1			c.118C>T	p.Q40X	12
Exon 2	$F1^{G}$	Heterozygous	c. 267G>A	p.W89X	This report
Intron 2	$F2^{T}$	Homozygous	c.442+1g>c	splice mutation	This report
Exon 3			c.529_533delATATT	p.I177_I178delfs179X	12
Exon 4	$F3^{S}$	Heterozygous	c.733_734delAT	p.M245fs246X	12, this report
Exon 6			c.1203delA	p.K401fsX	12
Intron 6	$F1^{G}$, $F4^{G}$	Heterozygous	c.1757-2a>g	p.E486fs508X	This report
Exon 9	$F4^{G}$	Heterozygous	c.1845_1846delGT	p.S616fs618X	This report
Exon 10	$F5^{SA}$	Homozygous	c.1951C>T	p.R651X	This report
Exon 11			c.2198T>G	p.L733X	12
Exon 14	$F3^{S}$	Heterozygous	c.2472insT	p.K825fs837X	This report
Exon 16			c.2842_2843insG	p.V948fsX	12
Exon 17	$F6^{T}$	Homozygous	c.3076insA	p.R1026fs1029X	This report
Exon 17	$F7^{T}$	Homozygous	c.3145_3146insCA	p.T1048fs1053X	This report
Exon 30	$F8^{G}$	Heterozygous	c.5255delT	p.F1752fs1765X	This report
Exon 30	$F9^{G}$	Heterozygous	c.5798delC	p.A1933fs1951X	This report
Exon 31			c.5974C>T	p.R1992X	12
Exon 32			c.6100C>T	p.R2034X	12
Exon 34			c.6451delG	p.A2151fsX	12
Exon 39			c.7029_7030insT	p.V2344fsX	12

[a]Origin: superscript G indicates Germany; superscript T indicates Turkey, superscript S indicates Spain; superscript SA indicates Saudi Arabia.

cDNA = complementary DNA.

PKA, LTK, MAP1A, MFAP1, MGA, FRMD5, EXDL1, NDUFAF1, NUSAP1, OIP5, PLDN, RHOV, TRIM69, SNAP23, KIAA1840, SPATA5L1, SPTBN5, SQRDL, TYRO3, UBR1, VPS18, ZFP106, ZFYVE19, ZSCAN29, according to the human genome nomenclature database)[15] were amplified by polymerase chain reaction (PCR). PCR products were cycle sequenced using the ABI Prism BigDye Terminator Cycle Sequencing Kit (version 1.1) and analyzed on an ABI 3100 Avant sequencer (Applied Biosystems, Foster City, CA). Each mutation identified within the 40 exons of the *KIAA1840* gene and their absence in any of 100 control chromosomes of Caucasian and/or Turkish origin was confirmed by restriction fragment length polymorphism when possible, or by sequencing or SNaPshot analysis (Applied Biosystems) of a second independent PCR product. Likewise, compound heterozygosity and cosegregation of the mutations with the phenotype in the respective families were demonstrated. To determine the effects of the splice-site mutation in Patients P1 and P4, we isolated messenger RNA from peripheral blood (PAXgene) of Patient P1 according to the manufacturers' recommendations. First-strand complementary DNA was synthesized using Superscript II (Invitrogen, La Jolla, CA). Subsequently, PCR products were generated with exonic primers 5F and 8R cloned into a pGem vector (Promega, Madison, WI); eight clones were sequenced.

Results

Mutational Analysis

In addition to previous microsatellite analysis, we confirmed linkage to the refined candidate region of SPG11 for the consanguineous Saudi-Arabian pedigree with ARHSP with TCC (Family F5; Fig 1A).[9,11] Following a positional candidate gene approach, no disease-associated mutations were detected in 30 genes tested from the SPG11 candidate region (see Patients and Methods). Finally, a total of 11 causal mutations were identified in the *KIAA1840* coding sequence (now designated *spatacsin*) in 3 consanguineous pedigrees from Turkey, 1 family from Saudi Arabia, 1 from Germany, and 4 sporadic patients of German or Spanish origin (Table 1). All mutations identified represent truncating mutations and include one previously reported and six novel frameshift mutations, as well as two novel nonsense mutations. Furthermore, we found

Table 2. **Summary of the Clinical Data**

Patient Data						MRI				SPRS		
Patient ID	Family ID(reference)	Position in Pedigree	Sex	Age at the Time of Examination (yr)	Age at Onset (yr)	MRI/CT	TCC	WML	Cortical Atrophy	Motor Function (total)	Spasticity and Weakness (total)	Total Score
P1	F1[10]		F	38	31	MRI	+	+	+	17	7	24
P2_1	F2[11]	*II-4 fam 3*	F	40	13	np				24	13	39
P2_2		*II-1 fam 3*	F	22	13	MRI	+	+	+	16	11	29
P2_3		*II-2 fam 3*	F	20	15	CT				16	10	28
P3	F3		M	19	11	MRI	+	+	+	13	3	21
P4	F4		M	33	8	MRI	+	−	+	16	8	24
P5_1	F5	*II-4*	M	26	17	MRI	+	+	+	17	11	29
P5_2		*II-6*	F	19	17	np						
P5_3		*II-7*	F									
P6_1	F6[11]	*II-1 fam 2*	F	30	16	MRI	+	+	+	23	12	38
P6_2		*II-2 fam 2*	F	28	17	np				21	12	36
P6_3		*II-3 fam 2*	F	26	13	np						
P6_4		*II-5 fam 2*	M	17	15	np						
P7_1	F7[11]	*IV-3 fam 1*	M	31	13	np				24	13	37
P7_2		*IV-10 fam 1*	M	26	12	np				24	13	40
P7_3		*IV-12 fam 1*	F	23	13	np				21	12	36
P7_4		*IV-13 fam 1*	F	21	13	MRI	+	+	+			
P8	F8		F	25	23	MRI	+	+	−	9	4	16
P9_1	F9[9]	*II-9*	F	34	25	MRI	+	+	+	18	11	40
P9_2		*II-10*	F	29	25	MRI	+	+	+	16	10	28

Pedigrees linked to SPG11: P1[10]; P2, P6, and P7[11]; P9[9]; and P5 (see Fig 1).

MRI = magnetic resonance imaging; SPRS = Spastic Paraplegia Rating Scale; CT = computed tomography; TCC = thin corpus callosum; WML = white matter lesion; np = not performed.

two different splice mutations (Table 1, Fig 1B) associated with the SPG11 phenotype (Figs 2A–C). Mutations are distributed throughout the entire *spatacsin* gene without obvious clustering in mutational hotspots (see Table 1).

The frameshift mutation c.733_734delAT, previously reported in a French patient, was observed in heterozygous state in a sporadic patient from Spain (Patient P3).[12] Two German patients of nonconsanguineous parents (Patients P1 and P4) were heterozygous for the novel base substitution at position −2 of the splice acceptor site of intron 6 (c.1757-2a>g; see Figs 2A, B). Another novel homozygous splice mutation of guanine to cytosine at position +1 of the splice donor site of intron 2 (c.442+1g>c) was identified in a consanguineous Turkish family (Family F2; see Fig 2C). For both splice mutations, the wild-type nucleotide at this position is highly conserved in the respective consensus sequence of mammalian splice sites. To confirm the consequences of the splice mutation c.1757-2a>g, we sequenced mature messenger RNA transcripts isolated from peripheral blood of Patient P1. Our data indicate for the mutant allele a skipping of exon 7, followed by the regular splicing of exon 8 sequences, resulting in a truncated protein p.E486fs508X (see Figs 2A, B). Sequence analysis of the entire *spatacsin* coding region and the flanking splice sites did demonstrate only one heterozygous mutation in Patient P8 (c.5255delT) and in Patient P9_1 and her sister P9_2 (c.5798delC), suggesting a heterozygous larger intragenic deletion or a heterozygous mutation in the regulatory sequence as a second disease-causing mutation in these patients. Both affected sisters of Family 9 share an identical haplotype.[9]

Clinical Characterization, Imaging, and Histopathological Findings

Detailed clinical information was available for 18 patients with identified *spatacsin* mutations (see Table 2). All patients fulfilled our inclusion criteria, that is, spasticity of the lower extremities, hyperreflexia, and positive extensor plantar responses. The mean age at onset of walking impairment as recognized by the patients was 16 years (range, 8–31 years). Detailed neurological examination showed predominantly bilateral proximal pronounced paresis of the lower limbs with a profound proximal spasticity and hyperreflexia of the lower limbs. All patients had extensor plantar responses. The gait was slow, spastic, and slightly ataxic. Interestingly, dysarthria was also observed as a common feature in SPG11 patients (85%). Two patients developed dysphagia and subsequent weight loss. Furthermore, a prominent bilateral amyotrophy of the hypothenar and thenar muscles was commonly present. Applying the SPRS to different cohorts with an approximate similar disease duration, we observed a faster progression of the SPRS score (mean, 31.2) compared with both a nonselected HSP cohort (mean, 20.0)[4] and a group of

Table 2. **Summary of the Clinical Data (continued)**

	Clinical Features									
Patient ID	Cognitive Deficit	Gaze-Evoked Nystagmus	Dysmetria/ Ataxia	Extrapyramidal Motor Signs	Muscle Wasting (upper limbs)	Muscle Wasting (lower limbs)	Neuropathy Sensory	Neuropathy Motoric	Amyotrophy	Pes Cavus
P1	+	+	+	−	+	+	+	+	+	−
P2_1	+	−	+	−	+	+	+	+	+	+
P2_2	+	−	−	−	−	−	−	+	−	−
P2_3	+	−	+	−	−	−	−	−	−	−
P3	+	+	+	−	−	−	−	+	−	+
P4	+	+	+	−	−	+	−	−	−	+
P5_1	+	−	+	−	+	+	+	+	+	+
P5_2										
P5_3										
P6_1	−	−	+	−	+	−	−	−	+	−
P6_2−	−	+	−	−	−	−	−	−	−	
P6_3	−		+				−	−	−	−
P6_4	+		−				−	−	−	−
P7_1	+	−	+	−	−	−	−	+	+	+
P7_2	+	−	+	−	−	−	−	−	−	−
P7_3	+	−	+	−	−	−	−	+	+	+
P7_4	+		+				−	+	+	+
P8	+	−	−	−	−	−	−	−	−	−
P9_1	+	+	+	+	−	+	+	+	+	−
P9_2	+	−	+	−	−	+	+	+	+	−

autosomal dominant HSP with confirmed SPG4 *(Spastin)* mutations (mean, 17.2; GeNeMove databank; Fig 3). This reflects a more severe motor impairment in this SPG11 cohort. In particular, the gait-related items (items 1–6) were severely increased with a median total score of 18.1 points determined after about 12 years of disease duration. General mental impairment of varying degree was noted in 83% of our cohort and confirmed in a subset of white patients as progressive with severe attentional deficits with intact long-term memory (Hamburger–Wechsler Intelligence Test for adults score, <70). MRI was performed for at least 1 affected member of each family (total: n = 10 patients) showing TCC associated with bilateral periventricular WM lesions and frontal cortical atrophy (Fig 4). Corpus callosum (CC) atrophy was pronounced in the rostral part in all patients with *spatacsin* mutations. In addition, progressive hypometabolism of the frontal cortex and thalamus was detected using ^{18}fluorodeoxyglucose positron emission tomography (P9_1; Fig 5). Furthermore, severe amyotrophy of thenar muscles was present in 45% of our patients associated with a mixed axonal demyelinating peripheral neuropathy (Figs 6A, B). Neuropathological analysis of the sural nerve (P9_1) showed hypomyelinization of large nerve fibers and loss of unmyelinated nerve fibers. In addition, accumulation of membranous material was noted in an unmyelinated axon (see Figs 6C, D). Single-voxel ^{1}H-proton magnetic resonance spectroscopy showed mild reduction of *N*-acetylaspartate acid in frontal WM, suggesting axonal loss with an increase of choline compatible with WM demyelinization in Patient P5_1. In addition, increased lactate level was observed both in frontal and parietooccipital cerebral regions, suggesting mitochondrial dysfunction (data not shown).

Natural Long-Term Course of One Characteristic SPG11 Patient

Patient P9_1 of German descent was first seen at the age of 26 and managed for more than 10 years. Initially, gait difficulties were noted when walking long distances associated with painful cramps. Maximum walking distance was about 1,000 m. Five years later, she was urged to retire from her position as a nurse assistant because of progressive motor impairment. Currently, the walking distance (item 1, SPRS, walking distance without pause) is less than 50 m. The walking speed is reduced to 180 seconds for 10 m (item 3, SPRS, maximum gait speed). Frequently, she is forced to use the wheelchair. In addition, urinary urge incontinence is increasingly prominent. The initial increased body mass index of 36 declined during the last year to 24 because of dysphagia. Currently, she receives antispastic treatment with baclofen (60 mg daily) and physiotherapy. During the 10-year period, the SPRS score increased from 32 to 40 points based on a reevaluation of the obtained measures for the motor function. Neurological examination showed the classic SPG

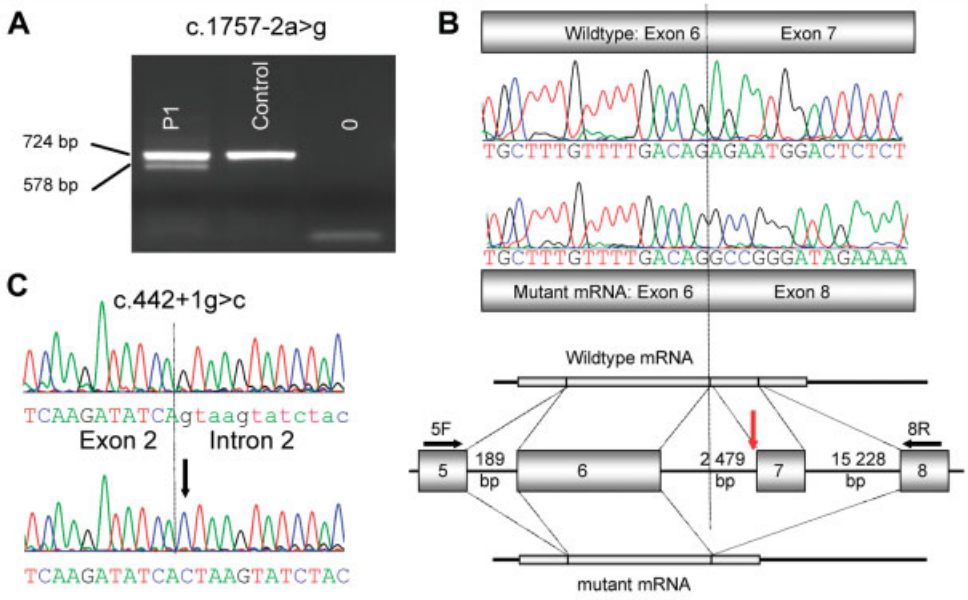

Fig 2. Identification of two spatacsin *splice mutations. (A) Messenger RNA (mRNA) analysis demonstrates the skipping of exon 7 in Patient P1 because of the splice-site mutation c.1757-2a>g. Electrophoretic separation of polymerase chain reaction (PCR) products obtained with primers located in exons 5 and 8 demonstrates the presence of the regular 724bp fragment and an additional smaller band of 578bp in the index case when compared with a control individual. (B) Sequence analysis of cloned PCR products after amplification of complementary DNA from a control (top lane) and Patient P1 confirming the skipping of exon 7 (bottom lane); schematic diagram of the genomic region and relative location of the exonic primers used for reverse transcriptase polymerase chain reaction and of the mutation* (red arrow). *(C) Homozygous base substitution c.442+1g>c at the donor site of intron 2 identified in Family F2 (bottom lane) when compared with a wild-type sequence (bottom lane).*

11 features: bilateral, proximal pronounced weakness of the lower limbs, profound proximal spasticity, hyperreflexia of the lower limbs, positive extensor plantar responses, gaze-evoked nystagmus, dysarthria, dysphagia, and palmar amyotrophy. Clinical MRI confirmed a thinning of the rostral part of the CC, which appeared as a thin band in the midsagittal T1-weighted images without obvious change of CC volume (see Figs 4A, C, E). Moreover, symmetric WM lesions were present in the axial fluid-attenuated inversion recovery sequences (see Figs 4D, F). Frontal lobe functions deteriorated and are paralleled by the progressive frontal cortical at-

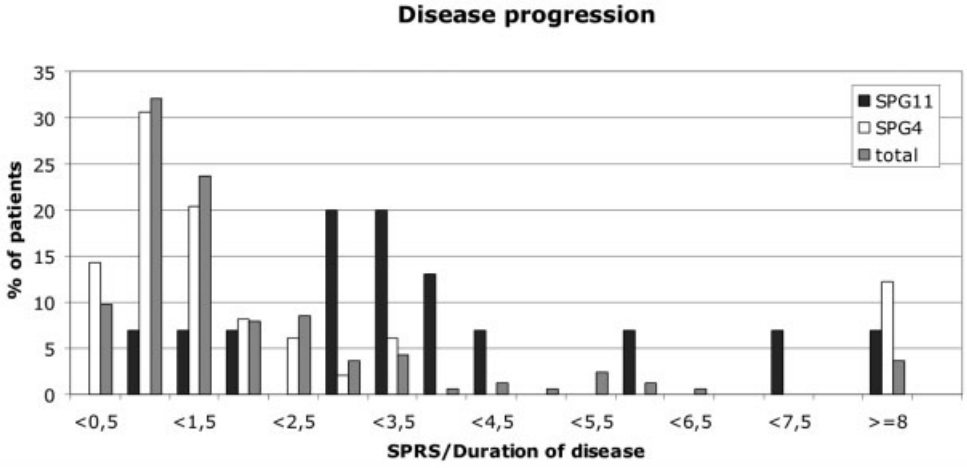

*Fig 3. Comparison of Spastic Paraplegia Rating Scale (SPRS) scores between SPG4 (*white bar, *n = 43), SPG11 (*black bar, *n = 15), and GeNeMove spastic paraplegia (SP) outpatients (*gray bar, *n = 165). The data are presented as SPRS score in relation to disease duration. Percentages of the patients/bin are presented. The SPRS for SPG11 is shifted toward higher scores, indicating a more severe motor impairment compared with SPG4 and the GeNeMove SP outpatient cohort.*

rophy (see Figs 4B, D, F) with a severe hypometabolism in the frontal cortex and the thalamus (see Fig 5).

Discussion

In patients with *spatacsin*-linked ARHSP with TCC, the neurodegenerative process is not restricted to primary motor neurons and the CST, but also affects major projections, in particular, mediating corticocortical connections via the CC. Additional cerebral regions such as the thalamus, periventricular WM, and *fasciculus gracilis* are affected. The presence of a severe palmar amyotrophy with mixed axonal demyelinating neuropathy indicates a degenerative process not solely restricted to the CNS.

Currently, about 60 patients linked to the SPG11 locus (15q13-15) have been described worldwide (see Winner and colleagues' review[10]). In addition, sporadic cases with genetically confirmed SPG4,[16,17] SPG21,[18] or SPG5a[19] also show TCC. However, the majority of families with ARHSP and TCC are associated with SPG11, probably accounting for 35 to 50% of all forms of ARHSP.[1,12,20] A clustering of genes associated with structural anomalies of the CC and/or motor and sensory neuropathy occurs in chromosomal region 15q14-q21.1 within an interval of 14Mb. Truncating and missense mutations in the gene for the potassium chloride cotransporter *SLC12A6 (KCC3)* in 15q14 cause the autosomal recessive Andermann syndrome

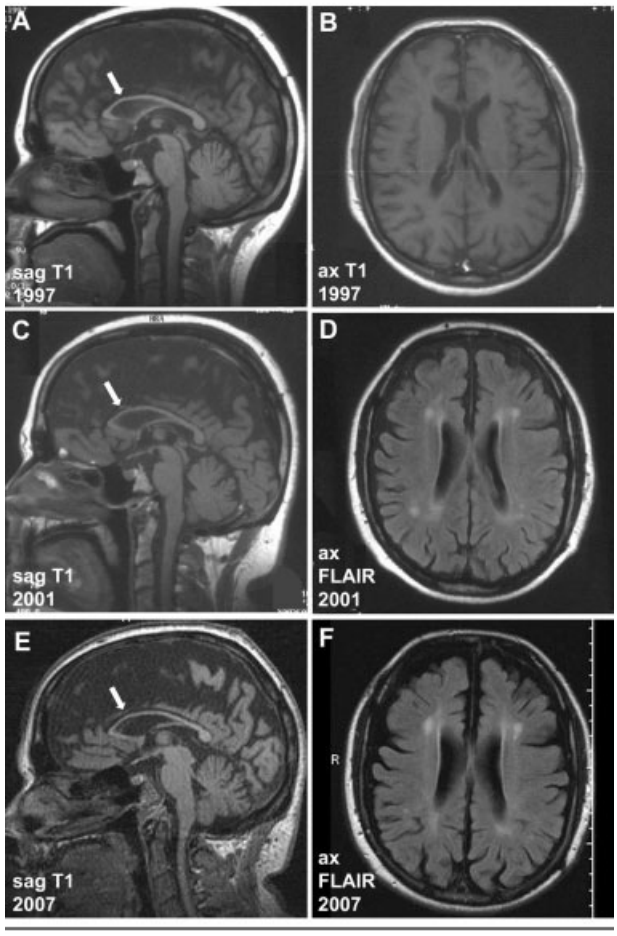

Fig 4. Long-term follow-up of cerebral magnetic resonance images in Patient P9_1. Sagittal (sag) T1-weighted images depict pronounced thinning of the rostral part of an atrophic corpus callosum (CC). Note that the atrophy of the CC is not progressive (A, 1997; C, 2001; E, 2007; arrows *indicate CC). Moreover, axial T1 (B) and axial fluid-attenuated inversion recovery (FLAIR) images (D, F) demonstrate progressive frontal atrophy with enlargement of the lateral ventricles and broadening of the interhemispheric sulcus; the latter (D, F) also demonstrate white matter lesions.*

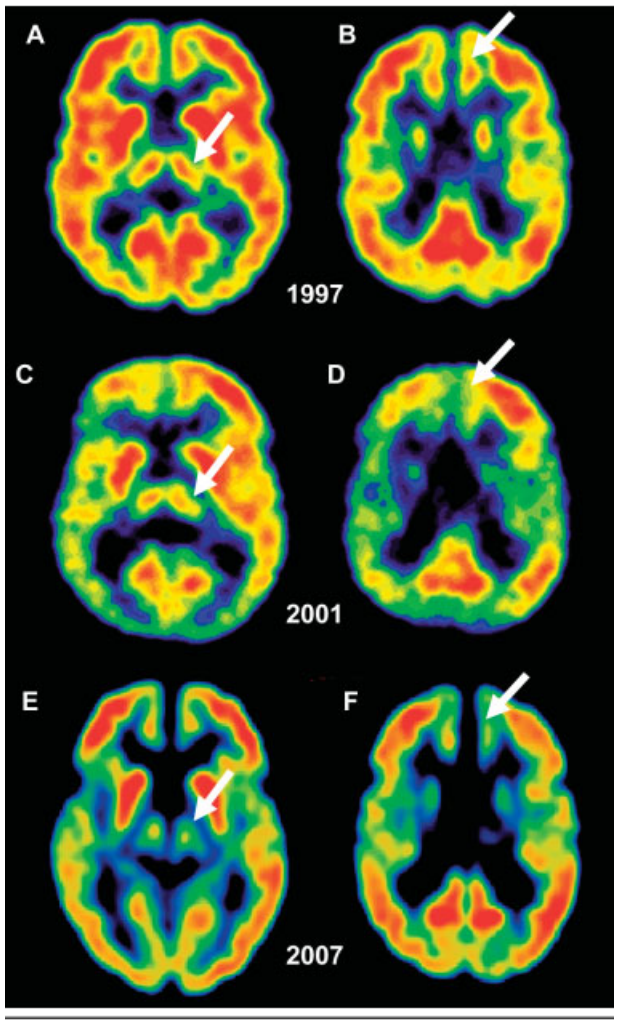

*Fig 5. Frontoparietal cortical and thalamic hypometabolism in ^{18}fluorodeoxyglucose positron emission tomography (FDG-PET). FDG-PET in the course of 10 years in Patient P9_1. PET images show a decrease in the thalamic metabolism (*arrows *in A, C, E). Moreover, metabolic decrease in the mediofrontal polar cortex (*arrows *in B, D, F) and in the cingulum is present. PET images were acquired using PET ECAT Exact 47 (1997, 2001) and Biograph 16 (2007; both Siemens, Erlangen, Germany).*

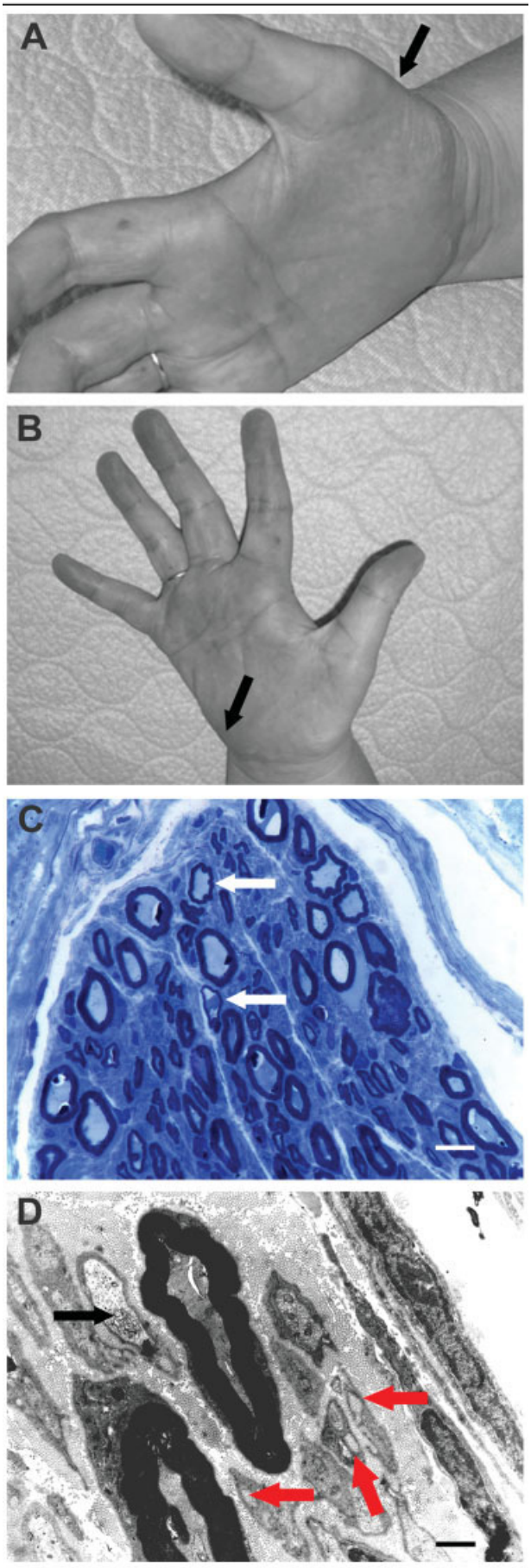

(MIM 218000), which is clinically characterized by early-onset and progressive peripheral neuropathy with agenesis of the CC.[21,22] ALS5 (MIM 602099), the major locus for autosomal recessive amyotrophic lateral sclerosis with a juvenile onset, has also been linked to this region.[23] Furthermore, based on linkage analysis of eight families from the United States and Europe, the SPG11 locus was originally defined between markers D15S1007 and D15S1012 in 15q14.[6] According to the current version of the gene map (ensemble current release 45, June 2007),[24] the *spatacsin* gene resides outside and approximately 6Mb distal to this originally defined SPG11 region. We speculated in our previous study refining the SPG11 locus[11] that this discrepancy may result from greater stringency of applied clinical inclusion criteria. A recombination event in a family with Andermann syndrome may have contributed to the initial definition of the distal border for the original SPG11 region.[6] Spatacsin is expressed ubiquitously in the rat nervous system but most prominently in the cerebellum, cerebral cortex, hippocampus, and pineal gland.[12] Its biological function is still unknown. The presence of at least one transmembrane domain suggests a function as receptor or transporter. Furthermore, overexpression of a green fluorescent protein-spatacsin fusion protein in COS-7 cells resulted in fluorescence even after methanol fixation, indicating an association of the protein to membranes.[12] Gene ontology analysis suggests for the spatacsin protein to confer both a catalytic (GO:0003824) and a ferric iron–binding activity (GO:0008199).[25] In silico analysis for functional protein domains is predicting the presence of a coiled coil domain (between amino acids 1563 and 1588; SMART),[26] a tightly associated bundle of long α helices, and the presence of an O-glycosyl hydrolase domain (between amino acids 482 and 490). These enzymes hydrolyze the glycosidic bond between two or more carbohydrates, or between a carbohydrate and a noncarbohydrate moiety (InterPro: IPR001360).[27] Besides spatacsin, glycoside hydrolase family 1 contains other proteins known to be involved in neurodegenerative disorders. For instance, mutations in the gene for

Fig 6. Severe SPG11 associated neuropathy in Patient P1. Note the amyotrophy of the thenar (arrow) *and hypothenar muscle (see* arrows *in A, B). Light (C) and electron microscopic (D) analysis of sural nerve biopsy. Several large myelinated nerve fibers* (red arrows) *show disproportionately thin myelin sheaths (C; semithin resin section, toluidine blue). Electron microscopy showed numerous nonmyelinating Schwann cells encircling bundles of collagen fibers* (white arrows) *indicative of a loss of unmyelinated nerve fibers. There is a prominent accumulation of pleomorphic membranous material in an unmyelinated axon* (black arrow) *compatible with disturbed axonal transport (D; ultrathin section). Scale bars = 20 μm (C); 2 μm (D).*

the lysosomal enzyme β-glucosidase cause the autosomal recessive disorder Gaucher syndrome.[28] In particular, the subacute neuropathic Gaucher syndrome type III (MIM 231000) is associated with a spastic paraparesis, cognitive deterioration, and seizures. Mutations in the gene for the lysosomal β-mannosidase have been associated with mental retardation and a progressive demyelinating peripheral neuropathy (MIM 248510).[29] In addition, spatacsin is predicted to contain an Intradiol ring-cleavage dioxygenase domain between amino acids 2104 and 2381. Dioxygenases mediate incorporation of both atoms of molecular oxygen into substrates, with Intradiol dioxygenases being involved in the degradation of aromatic compounds by cleaving the aromatic ring between two hydroxyl groups (InterPro: IPR000627).[27]

The most characteristic MRI feature of *spatacsin*-linked SPG11 is the marked thinning of the anterior part of the CC mostly sparing the splenium. The CC, the major commissure connecting both cerebral hemispheres, is formed between the 8th and 12th week of development, but MRI-based evidence indicates a continued myelinization of the axonal cytoskeleton up to the second decade of life.[30] The anatomic subregions of the CC (genu, body, isthmus, and splenium) are topographically organized belonging to the highest order-latest maturing neural network of the brain.[31] A strong myelinization is predominantly observed in the medial and posterior CC portion, to a lesser degree in the anterior CC portion, connecting higher cortical centers such as prefrontal or posterior parietal cortex.[32] ARHSP with TCC is characterized by a pronounced thinning of the anterior part of the CC, mostly paralleled by the progressive frontal cortical atrophy. In conjunction with recent studies, our data indicate no further progression of the CC thinning in advanced stages of the disease, but rather a progressive atrophy of the mediofrontal cortex.[33] In contrast, a progression of CC thinning was observed in a genetically mixed HSP population using MRI volumetry.[20]

In addition, bilateral periventricular WM changes are a characteristic MRI feature in the present *spatacsin*-linked SPG11 cohort. Notably, these subtle or diffuse signal alterations in supratentorial WM regions with increased signal intensity in T2-weighted images still require the exclusion of leukodystrophies such as adrenoleukodystrophy. Furthermore, the involvement of the thalamus in SPG11 has been frequently observed and may contribute to the cognitive deficit.[9,34] Our positron emission tomography studies in conjunction with the one ^{1}H-proton magnetic resonance spectroscopy indicate a progression of the metabolic dysfunction within the thalamic and frontal lobe regions. Another hallmark of *spatacsin*-linked SPG11 is a severe motor neuropathy leading to an amyotrophy in half of our patients. Sural nerve biopsy depicted a loss of unmyelinated nerve fibers and accumulation of pleomorphic membranous material in unmyelinated axons. These neuropathological alterations are unspecific but suggestive for a disturbed axonal transport. Spatacsin may play a role in the maintenance of both central and peripheral axons secondarily leading to loss of Betz and anterior horn cells. We hypothesize that the SPG11 phenotype results from the combined degeneration of central and peripheral axons associated with a neuronal loss within cortical and thalamic regions and in the spinal cord. Using the SPRS, we determined that the motor function is more severely affected in *spatacsin*-linked SPG11 compared with an SPG4-linked HSP cohort. This may be because of the involvement of the CNS and peripheral nervous system in this complicated HSP form. We propose that disturbed axonal transport processes may be the underlying mechanism for the neurodegenerative process in SPG11 involving the CST, CC, periventricular WM, and peripheral nerves. Future functional studies are needed to unravel the distinct role of spatacsin for maintaining long-projecting neurons in the CNS and peripheral nervous system.

The authors wish to dedicate this article to L. J. Thal, one of the pioneers in the field of neurodegenerative disorders.

This work was supported by the Tom Wahlig Foundation (Jena, Germany), the "Regensburger Forschungsförderung der Medizinischen Fakultät" (ReForM; University of Regensburg, Germany), the German Ministry of Education and Research (BMBF; B.W., G.U., J.W., U.H.) to GeNeMove (01GM0603), the German Leucodystrophy Network (LEUKONET; R.S., L.S., P.B., O.R.), the German academic exchange program (A.O., DAAD), and the Fondo Investigaciones Sanitarias (J.G., 02/0648, A.O., 07/0390).

We are grateful to the patients and their families for their participation in this study. We thank C. Mai, F. Renner, A. Milenkovic, B. Grigo, and A. Schuller for excellent technical assistance, and W. Schulte-Mattler, R. Luerding, E. Beck and H. Mader for neurophysiological and neuropsychological assessment of the German patients.

References

1. Fink JK. Hereditary spastic paraplegia. In: Rimoin DL, Emery AEH, eds. Emery & Rimoin's Principles and Practice of Medical Genetics. 5th ed. Philadelphia: Churchill Livingstone Elsevier, 2007; 2771–2801.
2. Reid E. Science in motion: common molecular pathological themes emerge in the hereditary spastic paraplegias. J Med Genet 2003;40:81–86.
3. Behan WM, Maia M. Strümpell's familial spastic paraplegia: genetics and neuropathology. J Neurol Neurosurg Psychiatry 1974;37:8–20.
4. Schule R, Holland-Letz T, Klimpe S et al. The Spastic Paraplegia Rating Scale (SPRS): a reliable and valid measure of disease severity. Neurology 2006;67:430–434.
5. Harding AE. Classification of the hereditary ataxias and paraplegias. Lancet 1983;1:1151–1155.
6. Martinez Murillo F, Kobayashi H, Pegoraro E, et al. Genetic localization of a new locus for recessive familial spastic paraparesis to 15q13–15. Neurology 1999;53:50–56.

7. Shibasaki Y, Tanaka H, Iwabuchi K, et al. Linkage of autosomal recessive hereditary spastic paraplegia with mental impairment and thin corpus callosum to chromosome 15q13–15. Ann Neurol 2000;48:108–112.
8. Casali C, Valente EM, Bertini E, et al. Clinical and genetic studies in hereditary spastic paraplegia with thin corpus callosum. Neurology 2004;62:262–268.
9. Winner B, Uyanik G, Gross C, et al. Clinical progression and genetic analysis in hereditary spastic paraplegia with thin corpus callosum in spastic gait gene 11 (SPG11). Arch Neurol 2004; 61:117–121.
10. Winner B, Gross C, Uyanik G, et al. Thin corpus callosum and amyotrophy in spastic paraplegia—case report and review of literature. Clin Neurol Neurosurg 2006;108:692–698.
11. Olmez A, Uyanik G, Ozgul RK, et al. Further clinical and genetic characterization of SPG11: hereditary spastic paraplegia with thin corpus callosum. Neuropediatrics 2006;37: 59–66.
12. Stevanin G, Santorelli FM, Azzedine H, et al. Mutations in SPG11, encoding spatacsin, are a major cause of spastic paraplegia with thin corpus callosum. Nat Genet 2007;39:366–372.
13. Chi CS, Mak SC, Schian WJ, Chen CH. Oral Glucose lactate stimulation test in mitochondrial disease. Pediatr Neurol 1992; 8:445–449.
14. Gempel K, Kiechl S, Hofmann S, et al. Screening for carnitine palmitoyltransferase deficiency by tandem mass spectrometry. J Inherit Metab Dis 2002;25:17–27.
15. Wain HM, Lush MJ, Ducluzeau F, et al. Genew: the Human Gene Nomenclature Database, 2004 updates. Nucleic Acids Res 2004;32:D255–D257.
16. Orlacchio A, Kawarai T, Totaro A, et al. Hereditary spastic paraplegia: clinical genetic study of 15 families. Arch Neurol 2004;61:849–855.
17. Alber B, Pernauer M, Schwan A, et al. Spastin related hereditary spastic paraplegia with dysplastic corpus callosum. J Neurol Sci 2005;236:9–12.
18. Simpson MA, Cross H, Proukakis C, et al. Maspardin is mutated in mast syndrome, a complicated form of hereditary spastic paraplegia associated with dementia. Am J Hum Genet 2003;73:1147–1156.
19. Al-Yahyaee S, Al-Gazali LI, De Jonghe P, et al. A novel locus for hereditary spastic paraplegia with thin corpus callosum and epilepsy. Neurology 2006;66:1230–1234.
20. França MC, D'Abreu A, Maurer-Morelli CV, et al. Prospective neuroimaging study in hereditary spastic paraplegia with thin corpus callosum. Mov Disord 2007;22:1556–1562.
21. Howard HC, Mount DB, Rochefort D, et al. The K-Cl cotransporter KCC3 is mutant in a severe peripheral neuropathy associated with agenesis of the corpus callosum. Nat Genet 2002;32:384–392.
22. Uyanik G, Elcioglu N, Penzien J, et al. Novel truncating and missense mutations of the KCC3 gene associated with Andermann syndrome. Neurology 2004;66:1044–1048.
23. Hentati A, Ouahchi K, Pericak-Vance MA, et al. Linkage of a commoner form of recessive amyotrophic lateral sclerosis to chromosome 15q15–q22 markers. Neurogenetics 1998;2:55–60.
24. Hubbard TJP, Aken BL, Beal K, et al. Ensembl 2007. Nucleic Acids Res 2007;35:D610–D617.
25. The Gene Ontology Consortium. Gene Ontology: tool for the unification of biology. Nat Genet 2000;25:25–29.
26. Letunic I, Copley RR, Pils B, et al. SMART 5: domains in the context of genomes and networks. Nucleic Acids Res 2006;34: D257–D260.
27. Mulder NJ, Apweiler R, Attwood TK, et al. New developments in the InterPro database. Nucleic Acids Res 2007;35:D224–D228.
28. Jmoudiak M, Futerman AH. Gaucher disease: pathological mechanisms and modern management. Br J Haemat 2005;129: 178–188.
29. Kleijer WJ, Hu P, Thoomes R, et al. Beta-mannosidase deficiency: heterogeneous manifestation in the first female patient and her brother. J Inherit Metab Dis 1990;13:867–872.
30. Keshavan M, Diwadkar VA, DeBellis M, et al. Development of the corpus callosum in childhood and adolescence and early adulthood. Life Sci 2002;70:1909–1992.
31. Pujol J, Vendrell P, Junque C, et al. When does the human brain development end? Evidence if the corpus callosum growth up to adulthood. Ann Neurol 1993;34:71–75.
32. von Richthofen S, Tabrizian S, Grabe HJ, Meyer B-U. Interhemispheric transfer and its implications for neurology and psychiatry. Fortschr Neurol Psychiat 2003;71:449–457.
33. Okubo S, Ueda M, Kamiya T, et al. Neurological and neuroradiological progression in hereditary spastic paraplegia with a thin corpus callosum. Acta Neurol Scand 2000;102:196–199.
34. Ohnishi J, Tomoda Y, Yokoyama K. Neuroradiological findings in hereditary spastic paraplegia with a thin corpus callosum. Acta Neurol Scand 2001;104:191–192.